



Bader S. Alshammari and Dipan J. Shah

Abstract

Cardiac magnetic resonance (CMR) imaging plays a pivotal role in the investigation and diagnosis of cardiac masses. In this chapter, we will present some illustrative cases.

Keywords

Cardiac magnetic resonance (CMR) imaging • Tumor • Thrombus • Mass

Introduction

Primary cardiac tumors are uncommon (0.02–3%) [1, 2]. Cardiac masses and pseudomasses represent a diagnostic challenge to multiple imaging modalities. Echocardiography, cardiac magnetic resonance (CMR), and computed tomography (CT) are very important for detection of cardiac masses. Most primary cardiac tumors are benign [1]. Atrial myxoma is a benign tumor and by far the most common primary cardiac tumor while the majority of primary malignant cardiac tumors are angiosarcomas in adults or rhabdomyosarcomas in children. It is important to remember that cardiac metastases are 10–40 times more frequent than primary cardiac tumors, melanoma being the most common tumor preferentially metastasize to the heart [2].

Most cardiac masses are initially detected by echocardiography, which is a first line modality for imaging of the heart for a variety of conditions. However, echocardiography has several limitations: poor image quality in those with difficult acoustic windows, limited field of view, and limited tissue characterization [1, 2]. Cardiac MR (CMR) has become the modality of choice in this setting because of its excellent spatial resolution, ability to obtain multiple imaging planes, precise localization, and excellent tissue characterization

which allows a more comprehensive characterization of the mass and aids in generation of a differential diagnosis.

Role of CMR in the Evaluation of Cardiac Masses

The excellent soft tissue definitions that CMR provides allow clear delineation of the myocardium, pericardium and vascular structures, which facilitates the identification of abnormal mass. In addition, tissue characterization by CMR can assist in generating a differential diagnosis, and can distinguish different types of cardiac tumors. Tissue characterization is done by imaging the mass using a variety of different MR sequences (e.g. T1 weighted, T2 weighted, first pass perfusion or delayed contrast enhancement), which can assist in generating a differential diagnosis of cardiac masses (Table 12.1).

Typical magnetic resonance protocol used in assessment of cardiac masses consists of:

1. Multiplanar locator in order to know the position of the heart in the thorax.
2. Functional sequences, cine-MRI, of “bright blood” based on gradient echo, (fast imaging with steady-state precession, SSFP). They are sequences with mixed T2 and T1 weighting (T2/T1), with great differentiation in the signal intensity of the blood and the myocardium, which facilitates the detection of intracavitary lesion.

B.S. Alshammari, M.D. (✉) • D.J. Shah, M.D.
Houston Methodist DeBakey Heart and Vascular Center,
Houston, TX, USA
e-mail: badralshmary@gmail.com

Table 12.1 CMR characteristics of cardiac masses

| Cardiac mass | T 1 Weighted | T2 Weighted | Post contrast |
|--------------------------------|-------------------------------------|-------------------------------|-------------------------------|
| Myxoma | Isointense, heterogeneous | Hyperintense, heterogeneous | Heterogeneous enhancement |
| Papillary fibroelastoma | Isointense | Slightly hyperintense | Hyperintense |
| Rhabdomyoma | Iso- or hyperintense | Slightly hyperintense | Hypointense or isointense |
| Fibroma | Iso- or hyperintense | Hypointense | Hyperintense |
| Hemangioma | Isointense | Hyperintense or heterogeneous | Hyperintense or heterogeneous |
| Paraganglioma | Iso- or hypointense | Hyperintense | Hyperintense |
| Intravenous leiomyomatosis | Isointense | Isointense | Heterogeneous |
| Bronchogenic cyst | Hypointense | Hyperintense | None |
| Angiosarcoma | Isointense, with hyperintense areas | Iso- or hyperintense | Hyperintense |
| Undifferentiated sarcoma | Isointense | Isointense | Nonspecific |
| Rhabdomyosarcoma | Isointense | Isointense, heterogeneous | Central nonenhancing areas |
| Osteosarcoma | Hyperintense | Hyperintense | Nonspecific |
| Malignant fibrous histiocytoma | Isonintense | Hyperintense, heterogeneous | Nonspecific |
| Leiomyosarcoma | Isointense | Hyperintense | Nonspecific |
| Fibrosarcoma | Isointense, heterogeneous | Hyperintense | Central nonenhancing areas |
| Lymphoma | Hypo- or isointense | Hyperintense | Variable |

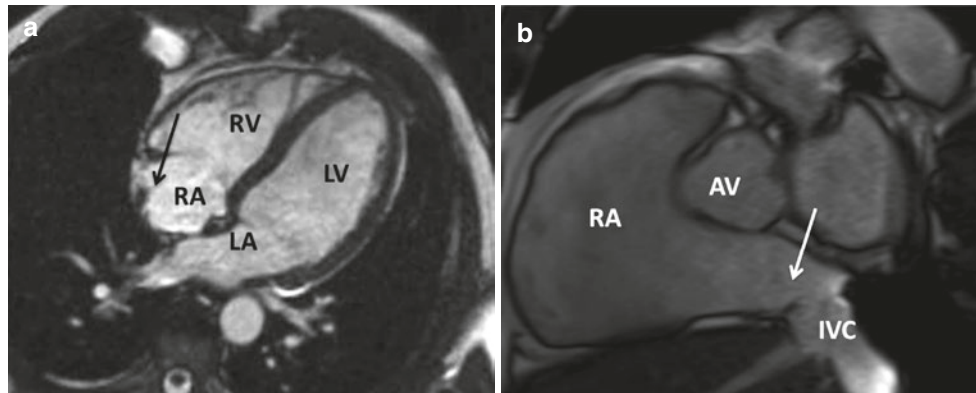


Fig. 12.1 (a) Cine steady-state free procession in the four-chambers view showing a prominent crista terminalis in the RA (*black arrow*)—a normal structure in the right atrium that can appear as a cardiac mass on echocardiography. (b) Cine steady-state free procession of Eustachian

valve showing a thin, mobile membrane (*white arrow*) extending from the inferior vena cava into the right atrium. *RV* right ventricle, *RA* right atrium, *LV* left ventricle, *LA* left atrium, *AV* aortic valve, *IVC* inferior vena cava

- Morphological and tissue characterization sequences based on spin echo. T1 and T2 weighted sequences will be obtained with or without fat suppression sequences.
- First-pass perfusion during rapid IV administration of gadolinium to assess for mass vascularity.
- Late gadolinium enhancement (LGE) sequences (T1-weighted sequences). They can be fast gradient echo or phase-sensitive inversion-recovery (PSIR) sequences. The inversion time for this sequence ranges from 150 to 300 ms. However, 500–600 ms inversion time is very useful to identify thrombi.

Cardiac Pseudomasses

There are a number of normal structures that are not true masses but can mimic a cardiac or paracardiac masses. The

most common of these is a right atrial pseudotumor produced by a prominent crista terminalis, which can appear as a right atrial mass on echocardiography (Fig. 12.1a).

A prominent Chiari malformation or Eustachian valve can also be mistaken as a right atrial mass; these can easily visualized by CMR (Fig. 12.1b).

Extracardiac structures that can simulate cardiac pathology include a large hiatal hernia that can compress the atria. CMR is superior to echocardiography in identifying hiatal hernia as a true extra-cardiac mass (Fig. 12.2).

Intracavitary Thrombi

The diagnosis of intracavitary thrombus may be suspected from echocardiographic findings (such as LV apical location or association with wall motion abnormality). However, it

can occur within any cardiac chamber. By far intracavitary thrombus is the most common intra-cardiac mass [3, 4]. Left atrial appendage thrombus is most commonly associated with atrial fibrillation [2].

Intraventricular thrombus usually occurs in the setting of cardiomyopathy, because decrease contractility predisposes to sluggish blood flow and can be a substrate for thrombus formation as shown in Fig. 12.3.

CMR enables thrombus to be detected based on intrinsic tissue characteristics related to avascular tissue composition. CMR is more sensitive and specific than echocardiography for detecting ventricular or atrial thrombi [3]. The sensitivity is significantly improved by administration of intravenous contrast material. Post-contrast delayed enhancement inversion recovery images with a long inversion time are exquisitely sensitive for detection of even small thrombi [5].

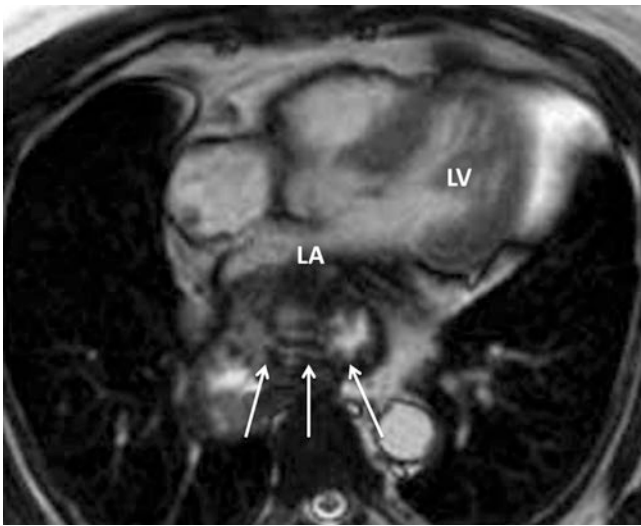


Fig. 12.2 Showing an axial Cine steady-state free procession in the chest with a large hiatal hernia (white arrows), which is compressing upon left atrium. LA left atrium, LV left ventricle

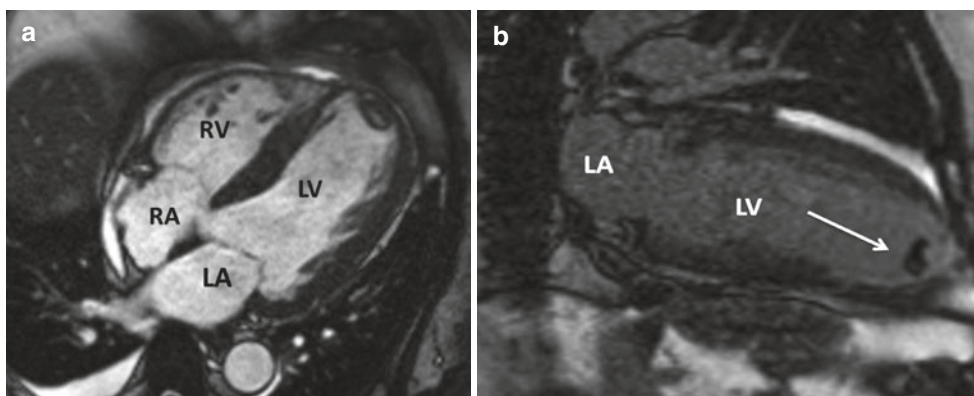


Fig. 12.3 A fifty-eight year-old male who presented with acute myocardial infarction and underwent angioplasty of LAD who underwent cardiac MRI. (a) Cine steady-state free procession showing a large apical thrombus. (b) Showing a thrombus (arrow) after gadolinium injection

The long inversion time allows recovery of signal by virtually all tissue except thrombus, which remains low in signal intensity and therefore dark on imaging as demonstrated in Fig. 12.3.

Benign Primary Cardiac Tumors

Benign cardiac tumors are usually classified pathologically according to histologic features. They can have an intracavitary location and be attached to endocardium or myocardium. They can also be intra-myocardial. Myxoma, papillary fibroelastoma, and lipoma are the most frequent ones.

Myxoma

Cardiac myxoma is the most frequent primary cardiac tumor (25–50%) [1]. The vast majority are sporadic and occur in adults between 40 and 70 years of age. They are usually asymptomatic or they can be associated with heart failure, systemic embolism, syncope or sudden death [6]. Nearly 7% of cardiac myxomas can exist as part of the carney complex which is an autosomal dominant syndrome characterized by myxoma, hyperpigmentation and extra-cardiac tumors [7].

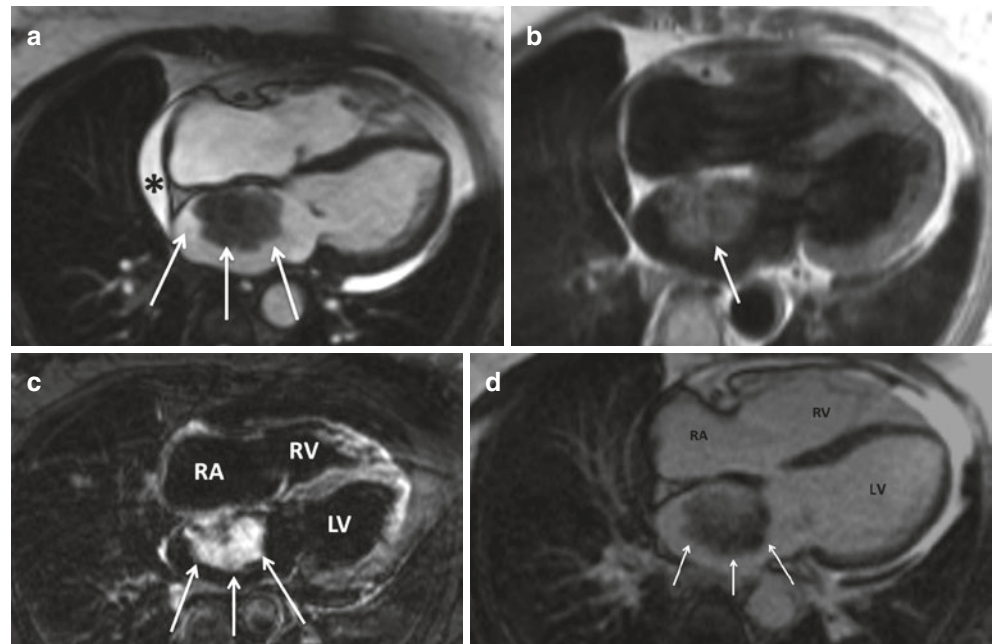
They are most commonly located in the left atrium (75%), they are usually attached by a pedicle to the interatrial septum, close to fossa ovalis and they can prolapse through the atrial-ventricular valves. Ventricular origin for myxoma is very rare (<2%) but can occur, as is right atrial origin [3].

Cardiac myxomas are heterogeneous masses of variable sizes (1–15 cm), due to the presence necrosis, calcification, bleeding, cystic formations or fibrosis [8].

CMR features of myxoma are shown in Fig. 12.4.

tion of the same patient performed 15 min after administration of gadolinium, using long inversion time (TI). LAD left anterior descending artery, RV right ventricle, RA right atrium, LV left ventricle, LA left atrium

Fig. 12.4 Myxoma in a 68-year-old asymptomatic male who underwent cardiac MRI. Cine steady-state free precession images in the four-chamber view, (a) demonstrates a well-outlined and intracavitary mass (white arrows) in the left atrium. Note a small pericardial effusion (asterisk). (b) In T1-weighted fast spin echo the mass can be identified in the left atrium well-outlined and of intermediate signal. LA myxoma appears hyperintense to myocardium on T2-weighted sequence (c); and heterogeneous enhancement after gadolinium injection (d). *RV* right ventricle, *RA* right atrium, *LV* left ventricle, *LA* left atrium



Papillary Fibroelastoma

Papillary fibroelastomas are benign avascular papillomas of the endocardium. They account for 10% of primary cardiac tumors [9, 10].

They are small (<1 cm), well-defined lesions, usually asymptomatic and usually detected incidentally by echocardiography that is performed for another indication. Most of them are usually located on the endocardial surface of the aortic (29%) or mitral (25%) valves [7].

CMR features of papillary fibroelastomas are shown in Fig. 12.5.

Lipoma

Cardiac lipomas are benign neoplasms composed of encapsulated mature adipose tissue, similar to extracardiac lipomas [3]. They can be detected at any age. Multiple cases have been described associated with tuberous sclerosis [11].

The most common location is the right atrium and the left ventricle. Other locations are cardiac valves, intramyocardial or pericardial [12].

Most lipomas do not cause any symptoms, but occasionally can lead to dyspnea if there is obstruction of blood flow, and/or arrhythmias if there is involvement of the cardiac conduction system [13, 14]. Given their fatty nature, cardiac lipomas are high in signal intensity on T1-weighted sequences with low signal intensity on fat saturation pulses sequences (e.g. T1 or T2-weighted spin echo).

CMR features of cardiac lipomas are shown in Fig. 12.6.

Lipomatous Hypertrophy of the Inter-Atrial Septum

Lipomatous hypertrophy of inter-atrial septum is not a true neoplasm. It is due to hyperplasia of otherwise normal fatty cells within the inter-atrial septum. The diagnosis is based on the finding of fatty deposits in the inter-atrial septum, resulting in a diameter exceeding 2 cm in the transverse dimensions. The exact etiology is unknown but it appears to be associated with obesity and advanced age. The exact incidence of this disorder is difficult to discern but incidences of lipomatous hypertrophy of the inter-atrial septum were 1% in autopsy series [19].

Lipomatous hypertrophy of the inter-atrial septum is associated with atrial arrhythmia [20].

CMR features of cardiac lipomatous hypertrophy of inter-atrial septum are shown in Fig. 12.7.

Fibroma

Cardiac fibromas are congenital neoplasms that typically affect children. However, 15% of cardiac fibromas occur in adults [15].

Approximately one-third of patients present with arrhythmias, one-third with heart failure or cyanosis, and one-third are detected incidentally [15].

They are well-circumscribed tumors located within ventricular myocardium as shown in Fig. 12.8.

The key findings are that they demonstrate reduced signal on T2-weighted imaging (due to their limited water content) and demonstrate very high signal intensity on LGE imaging (due to their high collagen content) [16].

CMR features of cardiac fibromas are shown in Fig. 12.8.

Fig. 12.5 Papillary fibroelastoma of the pulmonic valve demonstrated on cine steady-state free procession (a, b). Papillary fibroelastoma of the pulmonic valve demonstrating isointense signal on T1-weighted fast spin echo (c). After gadolinium injection imaging demonstrates intense contrast uptake by the mass (d). PA pulmonary artery, LA left atrium, LV left ventricle

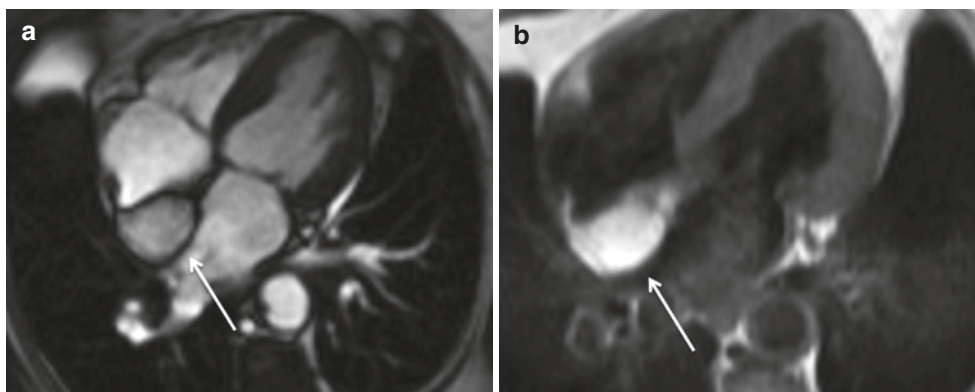
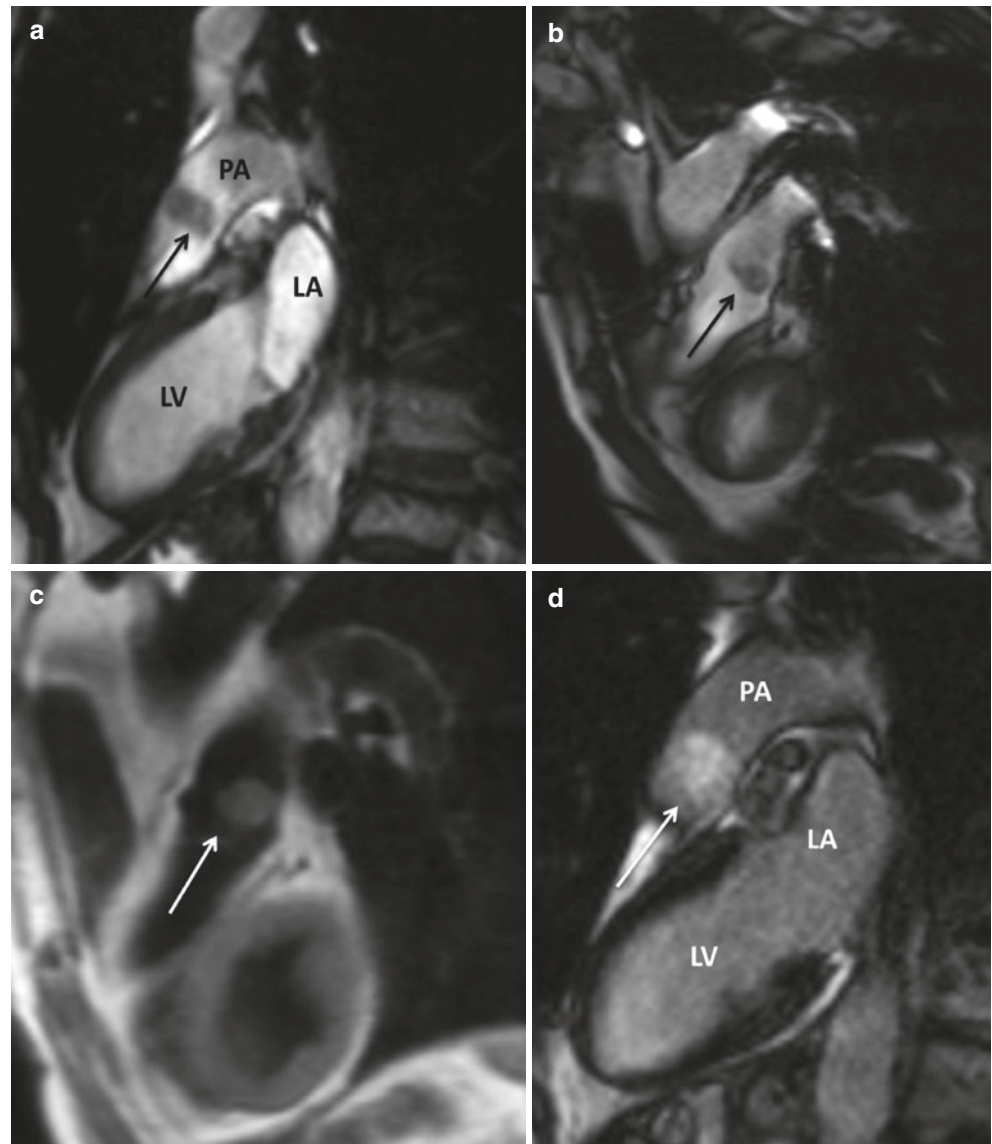


Fig. 12.6 Lipoma in a 53 year-old woman with incidental finding of a mass on echocardiography who underwent cardiac MRI. (a) Cine steady-state free procession demonstrating a well-defined uniformly high signal lesion within the inter-atrial septum (arrow). (b) Four-

Chamber T1-weighted fast spin echo image again showing the lesion as having uniformly high signal in keeping with a fat composition due to lipoma

Fig. 12.7 Cine steady-state free procession demonstrates lipomatous hypertrophy of the inter-atrial septum (**a**, *arrow*), and hyperintense on T1-weighted fast spin echo due to high fat content of the inter-atrial septum(**b**)

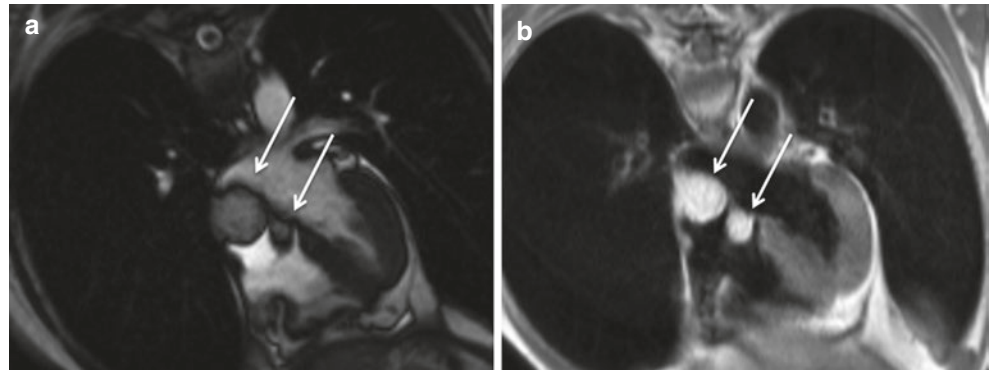
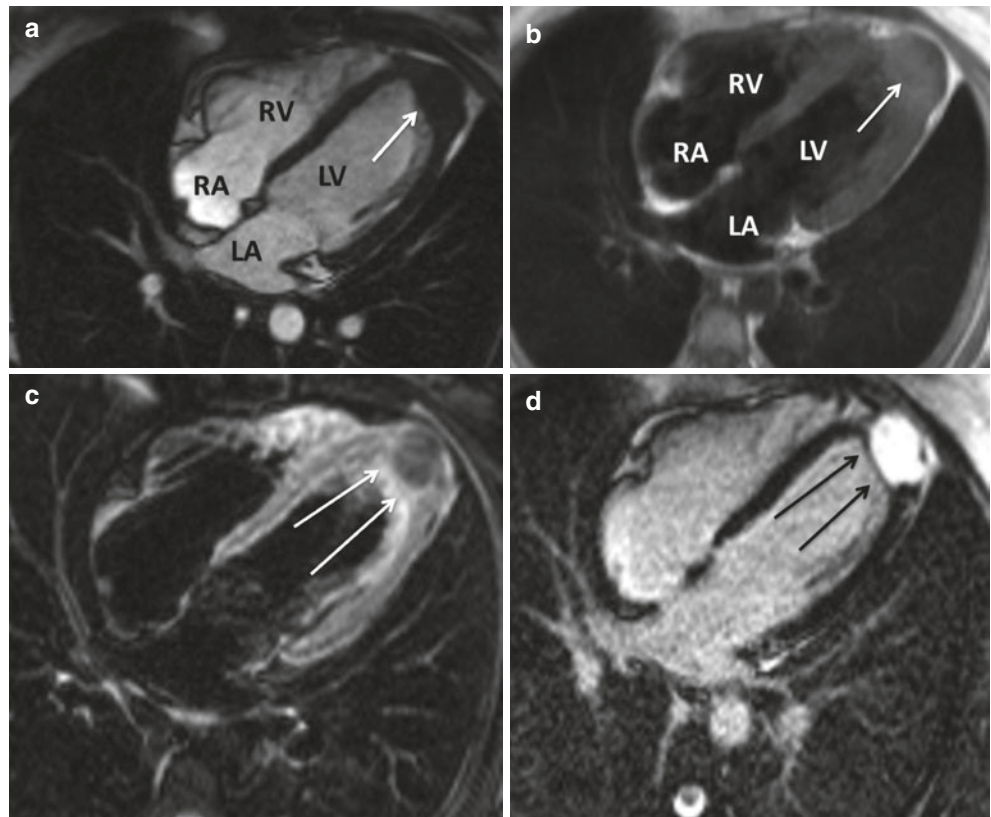


Fig. 12.8 Fibroma in asymptomatic 22 year-old female. Cine steady-state free procession in the four-chambers (**a**) and T-2 weighted imaging (**b**) demonstrating a homogenous myocardial mass in LV apex which appears isointense on T2-weighted imaging. Cardiac fibroma appears hypointense on T2-weighted images (**c**). The most characteristic feature of cardiac fibroma is diffuse homogeneous enhancement after gadolinium injection (**d**). *RV* right ventricle, *RA* right atrium, *LV* left ventricle, *LA* left atrium



Rhabdomyoma

Rhabdomyomas are the most frequent cardiac tumor in children. They are intramural tumors and can occur in isolation or associated with tuberous sclerosis [17]. They are usually asymptomatic but can cause obstruction of the ventricular outflow tract or arrhythmias [18].

CMR features of rhabdomyomas are described in Table 12.1 and in Fig. 12.9 [26].

Paraganglioma

Cardiac paragangliomas are exceptionally rare neuroendocrine neoplasms. Most of these lesions present with symptoms of catecholamine excess (hypertension, tachyarrhythmias, and heart failure). They usually occur between 10 and 60 years of age. Their usual location in the atria and at the root of the great vessels. They can be isolated or associated with paragangliomas in other locations (20%) [7].

CMR features of cardiac paragangliomas are shown in Fig. 12.10.

Fig. 12.9 Intramural left ventricular rhabdomyoma in a new born. (a) T1-weighted fast spin echo showing a large homogeneous isointense mass involving the LV wall. (b) Cine steady-state free procession in axial plane, showing the cardiac mass involving the interventricular septum. (c) Cine steady state free procession in four-chamber view, showing no intracardiac obstruction. (d) After gadolinium injection, no mass hyperenhancement is visible. *Ao* indicates aorta, *RA* right atrium, *RV* right ventricle, *LA* left atrium, *LV* left ventricle. Source: Reproduced with permission from [26] © 2011 Wolters Kluwer Health

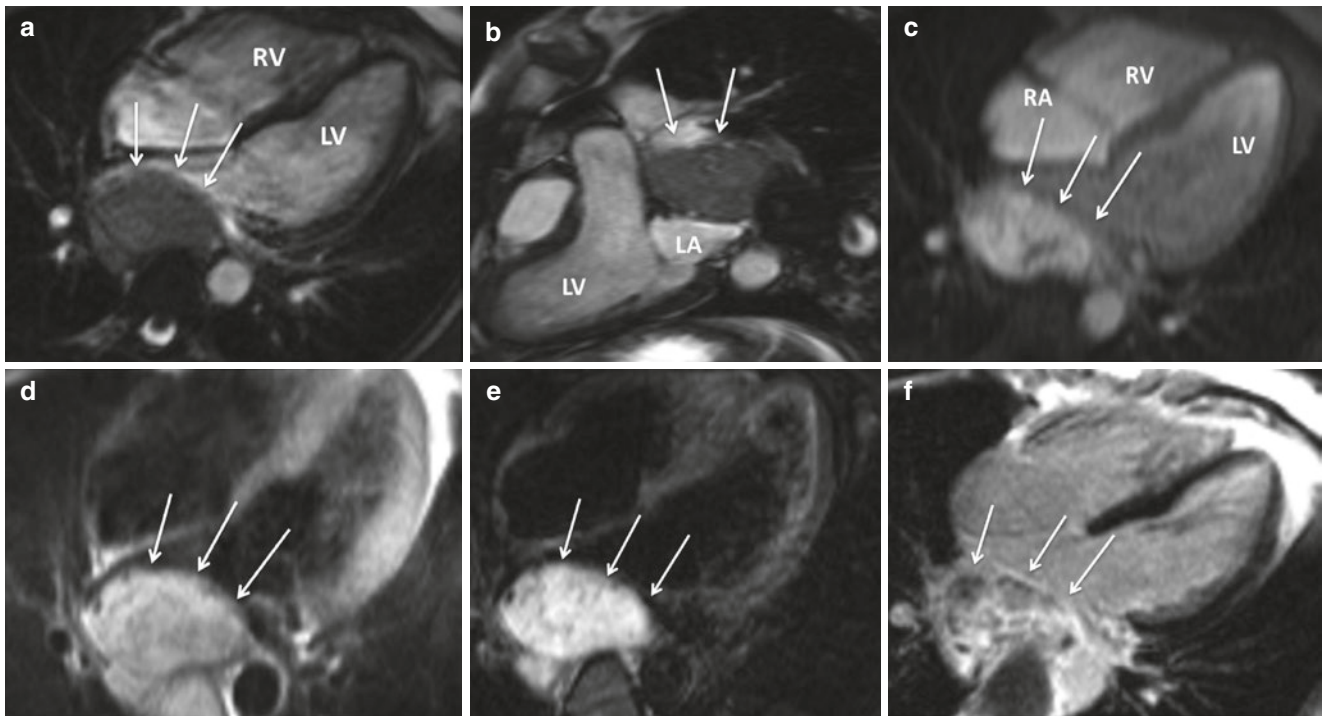
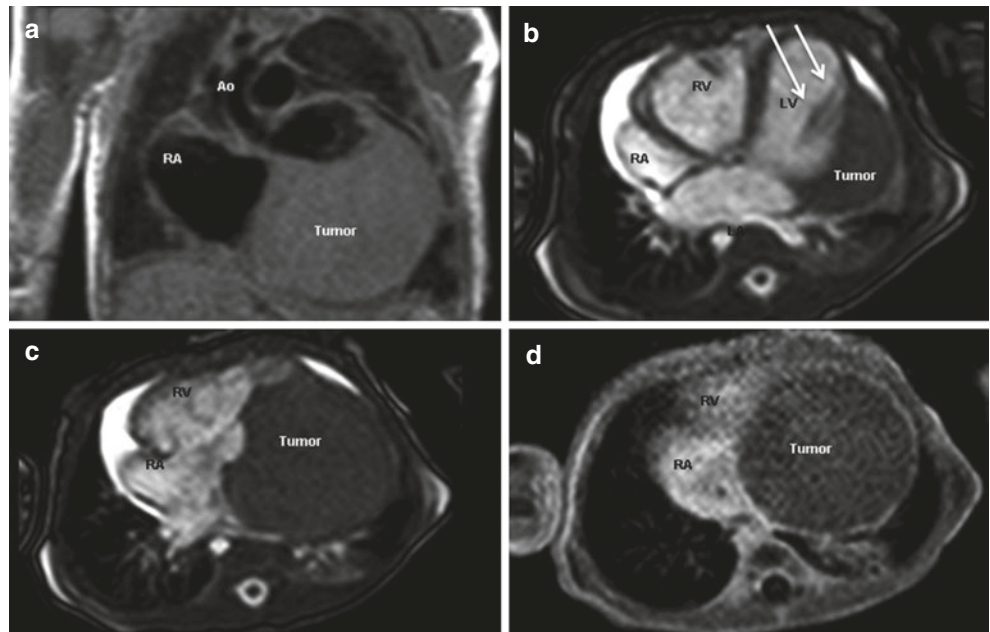


Fig. 12.10 Paraganglioma in a 42 year-old male with dyspnea who underwent cardiac MRI. Cine steady-state free procession demonstrating a large left atrial mass and extending along the inter-atrial septum (a, b). Paraganglioma on perfusion imaging (c) demonstrating first pass perfusion comparable to myocardium after gadolinium injection. The mass is isointense to myocardium on T1-weighted fast spin echo in

axial plane (d), hyperintense to myocardium on T2-weighted imaging in axial plane (e), and demonstrates heterogeneous uptake after gadolinium injection in axial plane (f). *RA* right atrium, *RV* right ventricle, *LV* left ventricle, *LA* left atrium, *SVC* superior vena cava

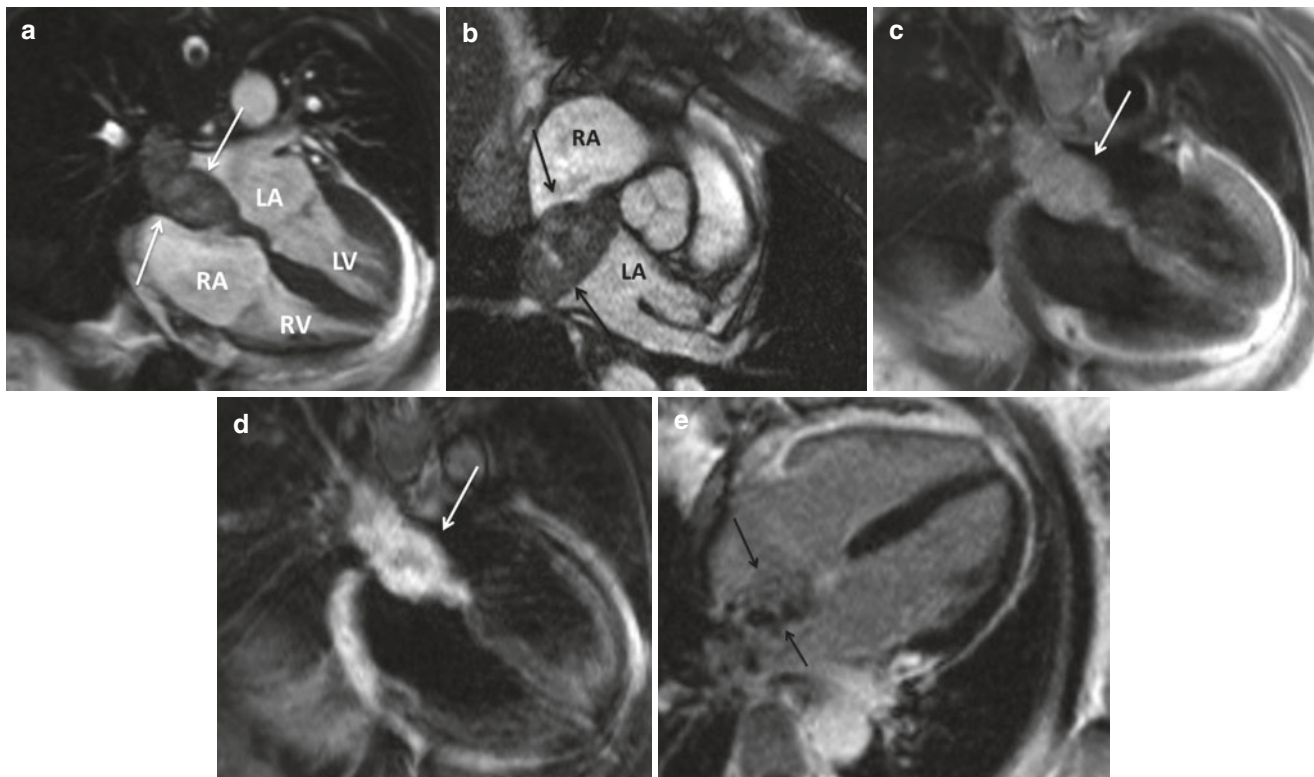


Fig. 12.11 Primary angiosarcoma in a 58 year-old male with dyspnea, peripheral edema and weight loss. (a) Cine steady-state free procession in axial plane shows a heterogeneous mass with invasion into the interatrial septum with partial obstruction of the SVC (b). Angiosarcoma

appears isointense on T1-weighted fast spin echo image (c), and hyperintense on T-2 weighted imaging (d). Primary angiosarcoma demonstrates heterogeneous uptake (e) after gadolinium injection (arrows). RV right ventricle, RA right atrium, LV left ventricle, LA left atrium

Malignant Primary Cardiac Tumors

Malignant tumors comprise approximately 25% of primary cardiac neoplasms [3]. They are classified by tissue type as mesenchymal (sarcoma), which represents the majority, or lymphoid with lymphoma making up most of the remainder. Imaging characteristics of malignant tumors are quite similar, with most lesions demonstrating invasion of surrounding structures and myocardium, poor border definition, and frequent coexisting pericardial effusion. Various cardiac sarcomas have many features in common with similar CMR features [3].

Angiosarcoma

Angiosarcoma is the most common form of cardiac sarcoma, accounting for approximately 40% of cases. Angiosarcoma has a predilection for the right atrium with more than 90% originating at this location [21].

Other forms of sarcomas (undifferentiated sarcomas, malign-

ant fibrous histiocytoma, osteosarcoma, leiomyosarcoma, or rhabdomyosarcoma) are bulky and infiltrating masses with a predilection to arise in the left atrium [22].

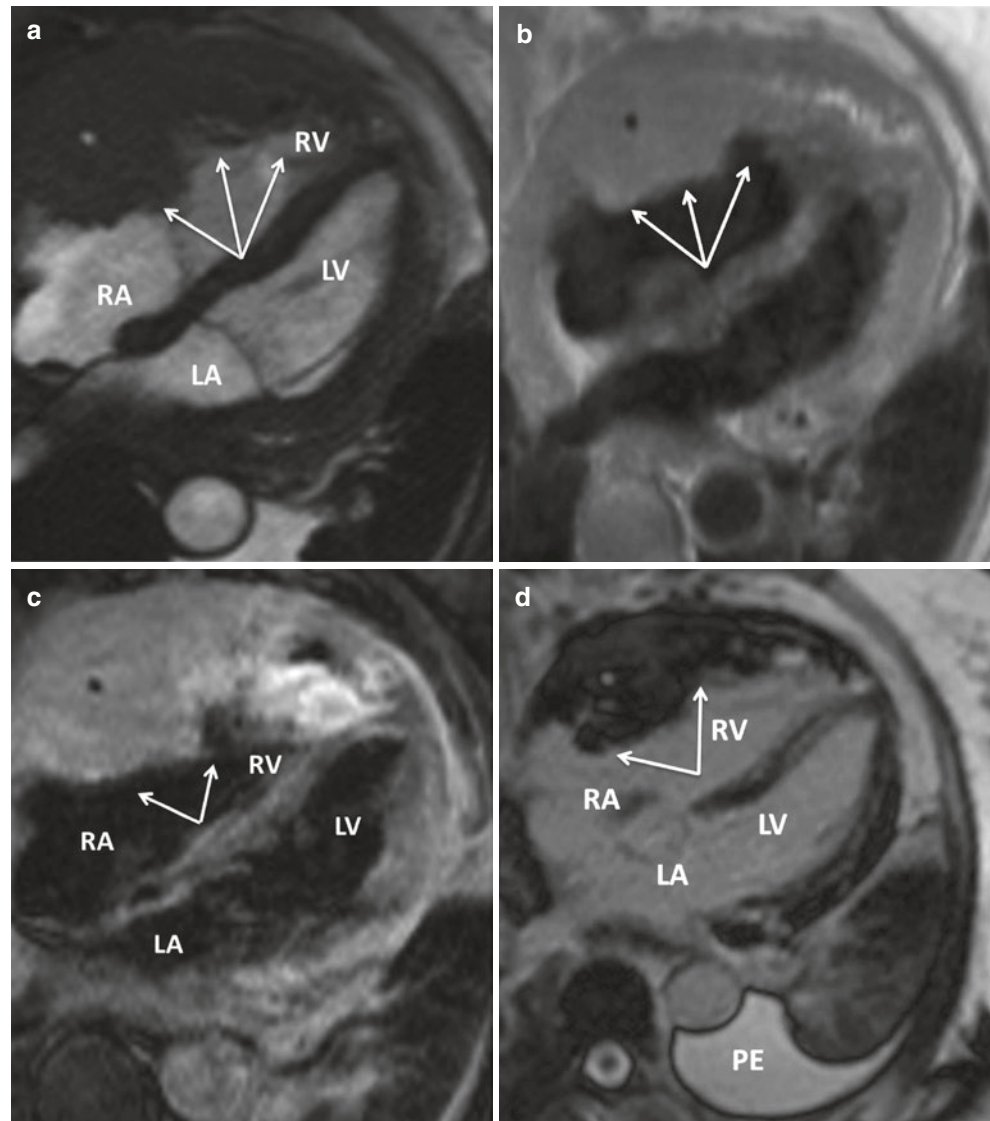
CMR features of angiosarcoma are shown in Fig. 12.11.

Lymphoma

Cardiac lymphomas are almost always aggressive B-cell lymphomas. These neoplasms have increased prevalence in immunocompromised patients, but also can occur in immunocompetent patients. The average age of presentation is approximately 58 years. Males appear to have a slight predominance [3]. Clinical features are typically of dyspnea, arrhythmia, superior vena cava obstruction or cardiac tamponade due to frequent involvement in the pericardium resulting in pericardial effusion. They are commonly involving right atrium, followed by right ventricle [7].

CMR features of cardiac lymphomas are shown in Fig. 12.12.

Fig. 12.12 Seventy-year-old male with cardiac B-cell lymphoma. Cine steady-state free precession in axial plane demonstrates a large tumor (arrows) originating in the right sided chambers not only involve cardiac chamber cavities but also within the myocardium (a). Cardiac lymphoma appears isointense T1-weighted fast spin echo imaging (b). Cardiac lymphoma demonstrates heterogeneous hyperintense on T-2 imaging (c) and heterogeneous uptake on post-contrast imaging (d). *RV* right ventricle, *RA* right atrium, *LV* left ventricle, *LA* left atrium, *PE* pleural effusion



Secondary Cardiac Tumors

Secondary cardiac tumors are 20 times more common than primary cardiac tumors [27]. Metastatic disease may result from contiguous extension, lymphangitic spread, transvenous route, or hematogenous spread [23]. Tumors metastasizing to the heart often involve the pericardium also. Metastatic malignant melanoma has the highest rate of car-

diac metastasis [24]. Metastases to the heart and pericardium are discovered at autopsy in 10–12% of all patients with malignancies [25].

Direct extension to involve the heart or the pericardium is often observed in lung carcinoma and breast. Hematogenous spread is usual for melanoma, leukemia, or sarcomas. CMR features of cardiac metastasis are shown in Fig. 12.13.

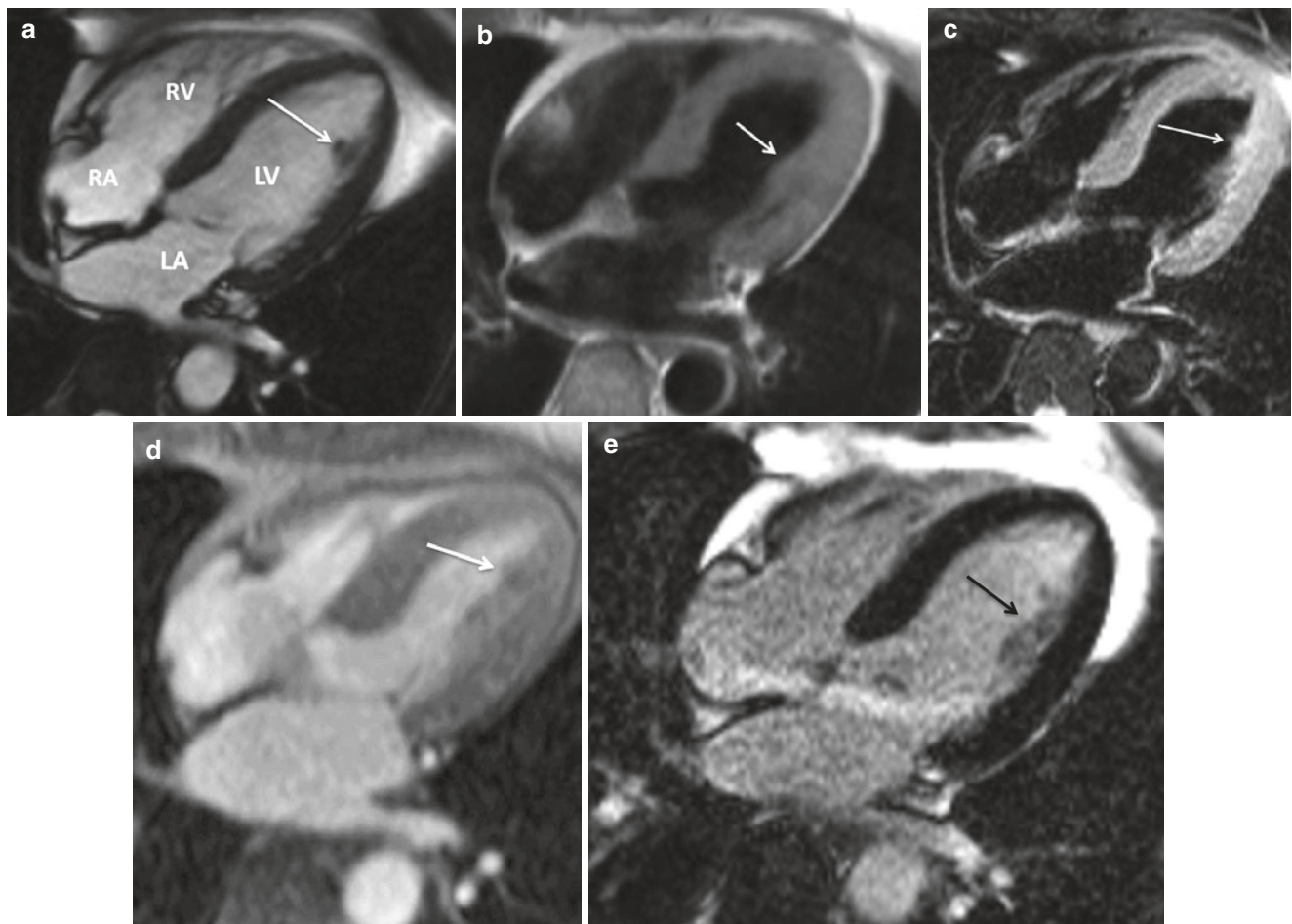


Fig. 12.13 Metastasis from skin melanoma in a 74 year-old female with palpitations demonstrating a well circumscribed intracavitary mass in LV on cine steady-state free precession in axial plane (*arrow*, **a**). The mass is isointense to myocardium on T1-weighted fast spin echo imaging (**b**). Also demonstrates a slight hyperintense lesion on T-2

weighted imaging (*arrow*, **c**) and hypoperfusion in comparison to myocardium on first pass imaging (*arrow*, **d**). Cardiac metastasis showing mild enhancement after gadolinium injection (*arrow*, **e**). *RV* right ventricle, *RA* right atrium, *LV* left ventricle, *LA* left atrium

References

- Motwani M, Kidambi A, Herzog BA, Uddin A, Greenwood JP, Plein S. MR imaging of cardiac tumors and masses: a review of methods and clinical applications. *Radiology*. 2013;268:26–43.
- Sparrow PJ, Kurian JB, Jones TR, Sivananthan MU. MR imaging of cardiac tumors. *Radiographics*. 2005;25:1255–76.
- Grizzard JD, Ang GB. Magnetic resonance imaging of pericardial disease and cardiac masses. *Magn Reson Imaging Clin N Am*. 2007;15(4):579–607, vi.
- Schwartzman PR, White RD. Imaging of cardiac and paracardiac masses. *J Thorac Imaging*. 2000;15(4):265–73.
- Weinsaft JW, Kim HW, Shah DJ, Klem I, Crowley AL, Brosnan R, James OG, Patel MR, Heitner J, Parker M, Velazquez EJ, Steenbergen C, Judd RM, Kim RJ. Detection of left ventricular thrombus by delayed-enhancement cardiovascular magnetic resonance prevalence and markers in patients with systolic dysfunction. *J Am Coll Cardiol*. 2008;52(2):148–57.
- Butany J, Nair V, Naseemuddin A, Nair GM, Catton C, Yau T. Cardiac tumours: diagnosis and management. *Lancet Oncol*. 2005;6:219–28.
- Araoz PA, Mulvagh SL, Tazelaar HD, Julsrud PR, Breen JF. CT and MR imaging of benign primary cardiac neoplasms with echocardiographic correlation. *Radiographics*. 2000;20:1303–19.
- Masui T, Takahashi M, Miura K, Naito M, Tawarahara K. Cardiac myxoma: identification of intratumoral hemorrhage and calcification on MR images. *AJR Am J Roentgenol*. 1995;164:850–2.
- Randhawa K, Ganeshan A, Hoey ET. Magnetic resonance imaging of cardiac tumors: part 2, malignant tumors and tumor-like conditions. *Curr Probl Diagn Radiol*. 2011;40:169–79.
- Burke A, Virmani R. Classification and incidence of cardiac tumors. In: Burke A, Virmani R, editors. *Tumors of the heart and great vessels: atlas of tumor pathology*, vol. 16. 3rd ed. Washington, DC: Armed Forces Institute of Pathology; 1996. p. 1–11.
- Ghadimi Mahani M, Lu JC, Rigsby CK, Krishnamurthy R, Dorfman AL, Agarwal PP. MRI of pediatric cardiac masses. *AJR Am J Roentgenol*. 2014;202:971–81.
- Rodríguez E, Soler R, Gayol A, Freire R. Massive mediastinal and cardiac fatty infiltration in a young patient. *J Thorac Imaging*. 1995;10:225–6.
- Zingas AP, Carrera JD, Murray CA III, Kling GA. Lipoma of the myocardium. *J Comput Assist Tomogr*. 1983;7(6):1098–100.

14. Conces DJ Jr, Vix VA, Tarver RD. Diagnosis of a myocardial lipoma by using CT. *AJR Am J Roentgenol*. 1989;153(4):725–6.
15. Burke AP, Rosado-de-Christenson M, Templeton PA, Virmani R. Cardiac fibroma: clinicopathologic correlates and surgical treatment. *J Thorac Cardiovasc Surg*. 1994;108:862–70.
16. Yan AT, Coffey DM, Li Y, Chan WS, Shayne AJ, Luu TM, Skorstad RB, Khin MM, Brown KA, Lipton MJ, Kwong RY. Images in cardiovascular medicine. Myocardial fibroma in gorlin syndrome by cardiac magnetic resonance imaging. *Circulation*. 2006;114(10):e376–9.
17. Nir A, Tajik AJ, Freeman WK, Seward JB, Offord KP, Edwards WD, et al. Tuberous sclerosis and cardiac rhabdomyoma. *Am J Cardiol*. 1995;76:419–21.
18. Tao TY, Yahyavi-Firouz-Abadi N, Singh GK, Bhalla S. Pediatric cardiac tumors: clinical and imaging features. *Radiographics*. 2014;34:1031–46.
19. Reyes CV, Jablockow VR. Lipomatous hypertrophy of the cardiac interatrial septum: a report of 38 cases and review of the literature. *Am J Clin Pathol*. 1979;72(5):785–8.
20. Hutter AM, Page DL. Atrial arrhythmias and lipomatous hypertrophy of the cardiac interatrial septum. *Am Heart J*. 1971;82(1):16–21.
21. Best AK, Dobson RL, Ahmad AR. Best cases from the AFIP: cardiac angiosarcoma. *Radiographics*. 2003;23(Spec no):S141–5.
22. Araoz PA, Eklund HE, Welch TJ, Breen JF. CT and MR imaging of primary cardiac malignancies. *Radiographics*. 1999;19(6):1421–34.
23. Chiles C, Woodard PK, Gutierrez FR, et al. Metastatic involvement of the heart and pericardium: CT and MR imaging. *Radiographics*. 2001;21(2):439–49.
24. Glancy DL, Roberts WC. The heart in malignant melanoma. A study of 70 autopsy cases. *Am J Cardiol*. 1968;21(4):555–71.
25. Abraham KP, Reddy V, Gattuso P. Neoplasms metastatic to the heart: review of 3314 consecutive autopsies. *Am J Cardiovasc Pathol*. 1990;3:195–8.
26. Padalino MA, Vida VL, Bhattarai A, Reffo E, Milanese O, Thiene G, Stellin G, Cristina Basso. *Circulation*. 2011;124:2275–7.
27. Lam KY, Dickens P, Chan AC. Tumors of the heart. A 20-year experience with a review of 12,485 consecutive autopsies. *Arch Pathol Lab Med*. 1993;117:1027–31.